The Canadian Mineralogist
Vol. 36, pp. 981-999 (1998)

APATITE AS A MONITOR OF FRACTIONATION, DEGASSING, AND METAMORPHISM IN THE SUDBURY IGNEOUS COMPLEX, ONTARIO

STEPHEN WARNER[1] AND ROBERT F. MARTIN[1]

Department of Earth and Planetary Sciences, McGill University, 3450 University Street, Montreal, Quebec H3A 2A7

ABDEL-FATTAH M. ABDEL-RAHMAN[1]

Department of Geology, American University of Beirut, Beirut, Lebanon

RONALD DOIG

Department of Earth and Planetary Sciences, McGill University, 3450 University Street, Montreal, Quebec H3A 2A7

ABSTRACT

Apatite occurs as an accessory phase throughout the Sudbury Igneous Complex (SIC), Ontario, a layered igneous complex consisting dominantly of norite, quartz gabbro, and granophyre. Apatite also is present in the overlying tuffaceous rocks of the Onaping Formation. Representative samples from three traverses (NW, NE, SW) across the complex have been studied in detail; the NW suite is the most pristine. Apatite is found primarily as a post-cumulus (or intergranular) phase, but becomes a cumulus mineral in the quartz gabbro. Despite textural signs of rapid growth, the apatite is homogeneous. It is F-rich; Cl and OH contents decrease from the base of the complex upward, as in several other layered intrusions. In the SIC, Cl and OH probably decreased relative to F upon vapor saturation of the evolving melt. The concentrations of *LREE*, up to 2 wt% $La_2O_3 + Ce_2O_3 + Nd_2O_3$, are highest in apatite near the base of the complex. The chondrite-normalized *REE* patterns and $^{87}Sr/^{86}Sr$ values (0.707–0.708) are similar in apatite from each rock type of the SIC. The complex evolved normally by fractional crystallization of a single batch of highly contaminated basic magma. The high initial $^{87}Sr/^{86}Sr$ values in apatite indicate that the relatively silica-rich basic magma had a substantial crustal component, or possibly consisted entirely of remelted crust. The apatite from the norite and that from the granophyre had a common magmatic source. Apatite from metamorphosed parts of the complex has significantly lower levels of Cl and *LREE*, compared to primary apatite from the NW section; furthermore, its $^{87}Sr/^{86}Sr$ value has been reset (up to 0.739) by exchange of strontium with adjacent K-rich minerals during recrystallization.

Keywords: apatite, Sudbury Igneous Complex, crystal chemistry, cumulates, contamination, trace elements, metamorphic recrystallization, Ontario.

SOMMAIRE

L'apatite forme un accessoire ubiquiste dans les roches du complexe igné de Sudbury, en Ontario, massif stratiforme de norite, de gabbro quartzifère et de granophyre. L'apatite est aussi présente dans les roches tuffacées de la Formation Onaping, qui recouvrent l'unité granophyrique. Nous avons étudié des échantillons représentatifs prélevés le long de trois coupes (nord-ouest, nord-est et sud-ouest) au travers du complexe igné. Les roches de la section nord-ouest semblent les plus intactes. L'apatite est surtout un minéral post-cumulatif (ou intergranulaire), mais devient une phase cumulus dans le gabbro quartzifère. L'apatite primaire est homogène, malgré les indications texturales d'une croissance rapide. De plus, il s'agit surtout de fluorapatite; les teneurs en Cl et OH diminuent vers le sommet du complexe, comme dans plusieurs autres massifs stratiformes. Il semble probable que cette diminution signale une perte de Cl et de H_2O suite à la saturation du magma en phase volatile, au cours de sa cristallisation. Les teneurs en terres rares légères, jusqu'à 2% en poids de $La_2O_3 + Ce_2O_3 + Nd_2O_3$, sont les plus élevées près de la base du complexe. Les spectres des terres rares normalisés par rapport aux chondrites et les valeurs de $^{87}Sr/^{86}Sr$ (0.707–0.708) de l'apatite se ressemblent dans chaque type de roche important. Le complexe de Sudbury aurait évolué par cristallisation fractionnée d'une seule venue de magma basique fortement contaminé. Les valeurs élevées du rapport initial de $^{87}Sr/^{86}Sr$ dans l'apatite témoignent de l'apport important d'une composante crustale dans le magma basique initial, relativement siliceux, ou

---

[1] *E-mail addresses*: slwarner@fort-frances.lakeheadu.ca, bob_m@geosci.lan.mcgill.ca, arahman@aub.edu.lb

même d'une origine entièrement crustale. L'apatite de la norite et celle du granophyre ont une source magmatique identique. L'apatite de la suite de roches prélevées dans le secteur sud-ouest et, à un degré moindre, dans le secteur nord-est, a perdu une quantité importante de Cl et de terres rares légères par rapport à l'apatite primaire, conservée dans le secteur nord-ouest. Les valeurs de $^{87}Sr/^{86}Sr$ ont aussi été ajustées à la hausse (jusqu'à 0.739) par échange du strontium avec des minéraux potassiques adjacents au cours de la recristallisation métamorphique.

Mots-clés: apatite, complexe igné de Sudbury, chimie cristalline, cumulats, contamination, éléments traces, recristallisation métamorphique, Ontario.

INTRODUCTION

Apatite is virtually the only volatile-bearing rock-forming mineral in stratiform mafic igneous complexes. As such, it is an indicator of halogen concentrations in the evolving melt, as revealed by the variation in its proportion of F, Cl and OH as a function of height above the basal contact. Here, we examine the chemical composition of the apatite, including its strontium isotope composition, along three stratigraphic sections through the enigmatic Sudbury Igneous Complex and associated tuffaceous rocks of the Onaping Formation, exposed near Sudbury, Ontario.

The Sudbury Igneous Complex displays many of the characteristics of a typical stratiform igneous body, but is unusual in many ways; its origin is still controversial. Major questions persist: (1) Is the structure the result of a meteor impact or an endogenic event? (2) Are the basic and felsic magmas cogenetic? (3) What is the link of the basic and felsic magmas with the magma that led to the overlying tuffaceous rocks of the Onaping Formation? (4) Is the source of the major batches of magma in the mantle, in the crust, or are both sources involved? (5) To what extent has regional metamorphic recrystallization affected the rocks exposed on the southern flank of the structure? The chemical composition of apatite, a relatively resistant accessory mineral present at all levels of the Sudbury Complex, is documented here to address some of these questions.

DESCRIPTION OF THE SUDBURY STRUCTURE

The Sudbury Structure, which hosts some of the richest Ni–Cu deposits in the world, is located in south-central Ontario, approximately 50 km north of Georgian Bay. This large elliptical structure (27 × 60 km) lies at the boundary between the Superior (Archean) and Southern (Proterozoic) provinces, and is 15 km northwest of the Grenville Front (Fig. 1). It was emplaced 1.85 Ga ago (Krogh *et al.* 1984). Gravity and seismic data indicate the lack of an obvious feeder dyke beneath the lopolithic structure (Deutsch & Grieve 1994).

The *Sudbury Igneous Complex* (SIC), found directly above the brecciated footwall rocks, locally pseudotachylite-bearing (Thompson & Spray 1994), is divided into the Sublayer and Main Mass, both attributed the same age (Naldrett & Hewins 1984, Naldrett *et al.* 1986). The Sublayer and the Footwall Breccia host the Ni–Cu deposits. The Sublayer is an inclusion-rich unit of variable thickness found at the base of the SIC (Contact Sublayer) and as dykes extending outward from the Sudbury Structure (Offset Sublayer). The Sublayer consists of blocks of mafic and ultramafic rocks, massive sulfide, and country rock in a matrix that ranges in composition from norite and gabbro (Contact Sublayer) to quartz diorite (Offset Sublayer). In the Contact Sublayer, sampled in this study, the matrix contains cumulus orthopyroxene and plagioclase, and intercumulus augite, quartz, alkali feldspar, sulfides, apatite, and secondary biotite.

The Main Mass of the SIC consists of norite (base), quartz gabbro and granophyre (top, Fig. 2). It is distinguished from the Sublayer by its higher content of quartz and the scarcity of inclusions. The *norite* consists of cumulus plagioclase and orthopyroxene, intercumulus augite, and a micrographic intergrowth of alkali feldspar and quartz, Fe-Ti oxides, and apatite. Secondary hornblende and biotite mantle the primary pyroxenes and opaque phases. Naldrett & Hewins (1984) defined variations in the composition of the norite from the North and South ranges on the basis of quartz content and concentration and composition of mafic minerals; oddly, the *mg#* [100 MgO/(MgO + FeO)] of both pyroxenes in the norite increases upward (60 to 70) from the base to an intermediate level, then decreases upward normally (70 to 62). The *quartz gabbro* is composed of cumulus plagioclase, augite, and orthopyroxene; intercumulus minerals include micrographically intergrown alkali feldspar and quartz, and secondary hornblende and biotite. The abrupt increase of Fe–Ti oxides and apatite within the quartz gabbro suggests that these minerals became cumulus phases near the top of the unit.

The *granophyre* (Fig. 2) consists of micrographically intergrown quartz and alkali feldspar, typically in "sunbursts" surrounding early-formed plagioclase, and intergranular minerals: biotite, hornblende, apatite, sulfides, and zircon. The high silica content of the granophyric layer (~65% SiO_2) is likely to have precluded the accumulation of phases by settling. Each unit of the SIC retains a dominantly igneous texture; metamorphic minerals, including amphiboles, epidote,

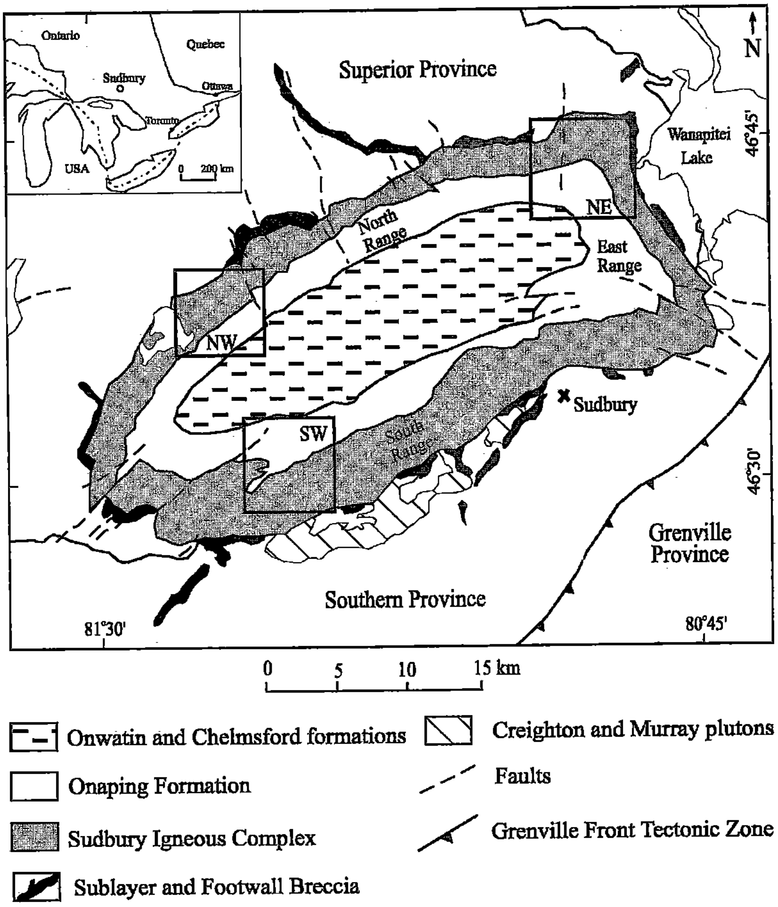

FIG. 1. The Sudbury Structure, as interpreted by Dressler *et al.* (1984); the inset shows its location in south-central Ontario. NW, NE, and SW are the areas selected for study. Road-side sampling (26 samples) was done at an interval of approximately 500 m, or whenever a new rock type was encountered. Eleven samples were taken from the NW section along Highway 144, from Windy Lake to Onaping Falls. Eight samples were taken from the NE section along Highway 545 north of Capreol, and a road heading east from Capreol. Seven samples were taken from the SW section along a road heading south from the eastern edge of Vermillion Lake toward the Lockerby mine. Samples of the Contact Sublayer are from the Levack West mine, in the NW section.

scapolite, biotite, chlorite, titanite, and recrystallized quartz, are more common in rocks from the South Range (Thomson *et al.* 1985).

The Onaping Formation (Whitewater Group), which overlies the Main Mass (Fig. 2), consists of either recrystallized impact-generated fall-back breccia (*e.g.*, Dressler *et al.* 1996) or reworked ash-flow tuff and lava composed of partly melted fragments of granitic and metasedimentary rock in a felsic, commonly carbonaceous matrix of devitrified glass shards and mineral fragments, formed by rapid cooling during a subaqueous impact (Gibbins *et al.* 1996). The presence of millimetric grains of diamond in the so-called Black Onaping unit provides firm evidence of a meteor impact (Masaitis *et al.* 1997). The Onaping Formation grades upward into sedimentary rocks of the Onwatin and Chelmsford formations, not sampled in this investigation.

The SIC differs from other stratiform igneous complexes in that it has higher levels of Si, K, light rare-earth elements (*LREE*), and lower levels of Ca and lower Na/K than basalts of similar *mg#* (Naldrett *et al.* 1986). Also, the SIC has a much larger volume of granophyric rocks (Naldrett & Hewins 1984) than could be expected by a combination of fractional crystallization and

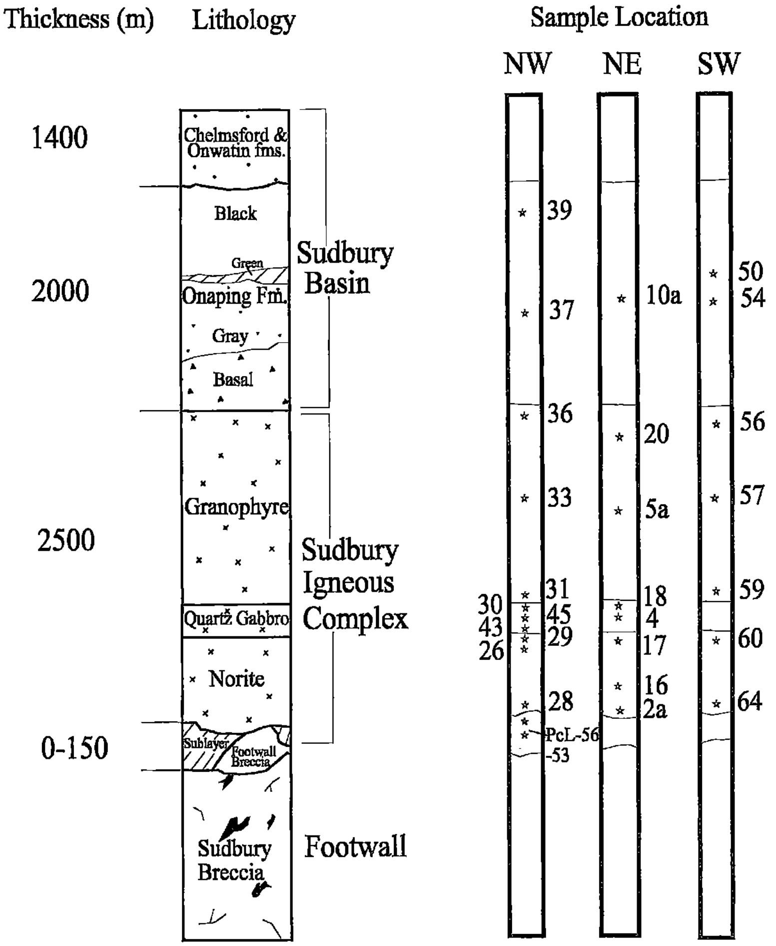

FIG. 2. Stratigraphic sequence of the Sudbury Structure on the undisturbed North Range. Position of samples is approximate, and the number beside each column is the sample number. Modified from Stöffler *et al.* (1994).

anatectic reactions along its external contact with the host rocks. Thus questions persist about the origin of the granophyre. The "reversal" in *mg#* found in ortho- and clinopyroxene may well be correlated with significant contamination toward the base. The SIC is now established as the result of a meteor impact on the basis of: (1) inferred circular shape prior to post-emplacement deformation, (2) shatter cones and strong brecciation of country rocks, (3) shock-metamorphic features in the basement rocks and in the Onaping Formation, including the presence of diamond, and (4) overturned collar rocks on the South Range (Peredery & Morrison 1984). In addition, studies of radiogenic isotopes (Faggart & Basu 1985, Naldrett *et al.* 1986, Walker *et al.* 1991, Dickin *et al.* 1992, Deutsch 1994) indicate a strong crustal signature in the mafic and felsic rocks and ores of the SIC, but questions remain as to the ultimate source of the magma(s).

Along the North Range (Fig. 1), units dip to the south at shallow angles, whereas in the South Range, units have been disrupted by south-dipping thrust faults or shear zones. Seismic reflection data (Milkereit & Green 1992) have shown the structure's elliptical outline and asymmetry in cross-section to be the result of northwest-directed thrust faulting; Fleet *et al.* (1987) suggested that the accompanying metamorphic recrystallization occurred in a single post-emplacement event. Thomson *et al.* (1985) reported that the regional metamorphic overprint was largely limited to the South and East ranges (upper greenschist to amphibolite facies), and faded northward. The 37 Ma Lake Wanapitei impact structure (Peredery & Morrison 1984) may have contributed to the deformation of rocks on the East Range. In contrast, rocks on the North Range, especially along the northwestern edge, are relatively unmodified (subgreenschist facies).

The age of metamorphism and deformation of the South Range is still being debated. It is likely that metamorphism took place soon after emplacement, during the Penokean orogeny (1.89–1.83 Ga: Bickford *et al.* 1986), a regional event considered responsible for greenschist-facies metamorphic assemblages in Huronian supracrustal rocks in the Southern Province, to the southeast of the Sudbury Structure. Regional metamorphism associated with the Grenville orogeny (approximately 1.0 Ga) is considered to have had little effect on the Sudbury Structure (*e.g.*, Dressler *et al.* 1984, Morris 1984, Peredery & Morrison 1984). In support of this proposal, Bethune & Davidson (1997) found Grenvillian metamorphic assemblages and corona development in mafic dykes of the Sudbury swarm (~1.24 Ga) restricted to within a few kilometers of the Grenville Front.

STRATIGRAPHIC DISTRIBUTION OF THE APATITE

In the bottom half of the SIC, apatite generally is a post-cumulus (or intergranular) accessory mineral, less than 1 vol.%, but it approaches 7% in the quartz gabbro. Selected whole-rock compositions and proportions of normative minerals in the SIC and Onaping Formation are listed in Table 1; the full dataset is available in Warner (1996). The bulk compositions and data in the literature point to an abrupt increase in the concentration of phosphorus (Fig. 3) within the quartz gabbro (up to 2.9 wt.% P_2O_5); the increase signals the first occurrence of cumulus apatite.

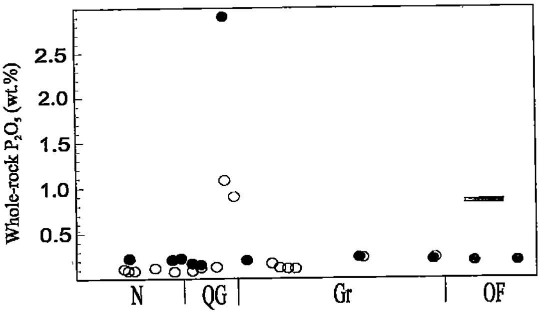

FIG. 3. Whole-rock P_2O_5 (wt.%) of samples from the NW section. N: norite, QG: quartz gabbro, Gr: granophyre, and OF: Onaping Formation. Filled symbols represent data from Warner (1996), and open symbols are data from Chai & Eckstrand (1993). Bar represents 450 m.

MORPHOLOGY OF THE APATITE CRYSTALS

Apatite was separated from norite, quartz gabbro and granophyre samples by initially breaking down the rock in a BICO jaw crusher, then by grinding between ceramic plates and sieving. The fraction coarser than 200 mesh was collected for heavy-liquid separation. A Frantz magnetic separator and further heavy-liquid separation removed most grains of mafic minerals, sulfides, and zircon. The apatite was then hand-picked.

The morphology of apatite separates reflects the order of crystallization (post-cumulus *versus* cumulus), and sample location (North *versus* South Range). Grains of cumulus apatite from the quartz gabbro collected from the North Range are stout and euhedral (Fig. 4a), whereas grains of post-cumulus apatite in norite samples are subhedral to anhedral, and finer grained (Fig. 4b). Grains of post-cumulus apatite from the South Range (Fig. 4c) are more strikingly anhedral, equant, scarcer, smaller and more heavily fractured than those from the North Range. If one accepts that the apatite originally crystallized under similar conditions on both flanks of the originally lopolithic complex, it seems necessary to appeal to post-crystallization events on the South Range (deformation, metamorphic recrystallization) to account for the smaller size and anhedral shape of the apatite crystals.

The following descriptions pertain to each rock type from the relatively unmetamorphosed NW section. Apatite in the *Contact Sublayer* occurs as stubby, subhedral to euhedral grains that attain 0.5 mm in length; most grains have an aspect ratio (l/w) of 3 to 4. As a post-cumulus phase, apatite is found in the intercumulus regions, along with augite, quartz, alkali feldspar, and secondary biotite. The apatite crystals are usually longer and stouter than that in the overlying norite, but most of the other intercumulus minerals in the Sublayer also are coarser than in the norite. Other factors being equal, the coarse grain-size is consistent with relatively slow crystallization of the intercumulus liquid in the deepest parts of the SIC.

Within the *norite*, apatite occurs as a post-cumulus phase; two generations are distinguishable on the basis of size and textural relationships. Early post-cumulus apatite (<1 vol.%) occurs as subhedral, elongate and slender (typically <200 μm in length, 20 < l/w < 25) crystals. In general, these are parallel to the plane of lamination defined by the cumulus plagioclase. Late post-cumulus apatite is less plentiful, up to 300 μm in length, subhedral or anhedral, and with an aspect ratio less than 10; the apatite fills voids between cumulus minerals. Both types of apatite are evenly scattered in the intercumulus regions along with augite, quartz, alkali feldspar, Fe-Ti oxides, and secondary biotite and hornblende. Apatite also is found within the overgrowth on cumulus plagioclase. The slender habit of early post-cumulus apatite, like the presence of an axial cavity (see below), may reflect relatively rapid crystallization from the interstitial liquid.

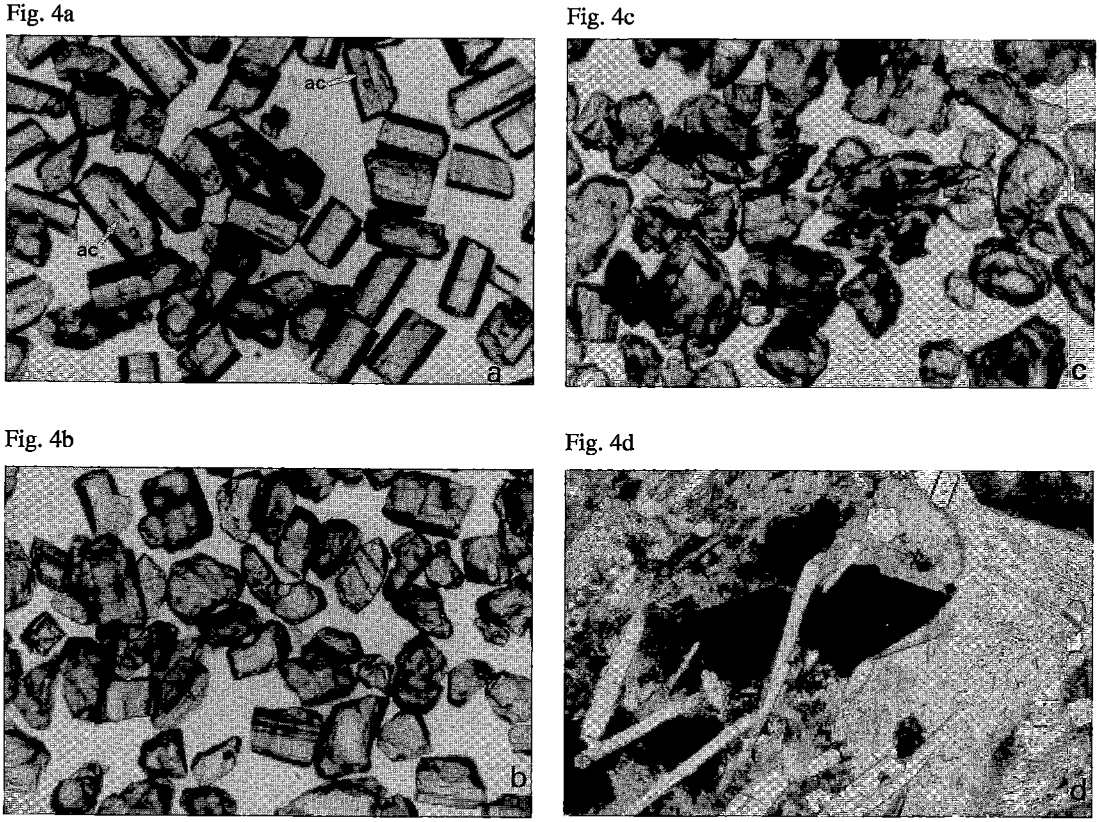

FIG. 4. Photomicrographs of apatite separates from the different rock types of the Main Mass from the NW and SW sections; sample numbers are shown in brackets. (a) Euhedral crystals of cumulus apatite from the quartz gabbro (30) on the North Range. Some of the crystals have an axial cavity (ac) parallel to the Z axis. (b) Subhedral to anhedral crystals of post-cumulus apatite from the norite (28) on the North Range. (c) Anhedral post-cumulus apatite from the norite (64) on the South Range. Note that here, all of the crystals are poorly developed and equant. Field of view for (a), (b), and (c) is 1 mm. (d) Photomicrograph (crossed nicols) of representative cumulus apatite from the quartz gabbro (30). Note the numerous cross-sections and prismatic sections. Field of view for (d) is 3 mm.

Apatite occurs as a cumulus phase only in the *quartz gabbro*. Cumulus apatite (Fig. 4d) forms subhedral to euhedral prisms up to 2 mm in length. Although in some cases the apatite is concentrated in layers and shows a close spatial relationship with Fe-Ti oxides, the cumulus apatite is usually scattered randomly throughout the thin sections. Also present in the quartz gabbro, but less prominent, are clusters of post-cumulus apatite crystals (usually less than 20–30 μm in length), associated with other intercumulus minerals.

In the *granophyre*, apatite is far less common (<1 vol.%) than in the underlying quartz gabbro (Fig. 3). The abundance of apatite decreases from the base of the granophyre toward the top. The intergranular apatite is mostly subhedral, with an average length between 100 and 200 μm (maximum 0.5 mm) and an aspect ratio ranging from 2 to 5. The crystals, in some instances, seem corroded or abraded. There also are smaller grains (<200 μm), which are more elongate ($20 < l/w < 25$). Pyroclastic rocks of the *Onaping Formation* contain even less apatite (<0.4 vol.%) than the underlying granophyre. The grains are typically less than 150 μm across and subhedral. The apatite found in the matrix and in devitrified lumps of melt are abraded, fragmented, and even pitted.

Some of the apatite separates have an axial cavity parallel to their Z axis (Fig. 4a), similar to that described by Drinkwater *et al.* (1990) in apatite from the Dufek

TABLE 1. WHOLE-ROCK COMPOSITION AND NORMATIVE MINERALOGY OF SELECTED SAMPLES FROM THE SUDBURY IGNEOUS COMPLEX AND ONAPING FORMATION

	NW Section								NE Section				SW Section				
Sample	28	29	45	30	33	36	37	38	16	4	18	20	64	62	58	56	LoD
Unit	N	N	QG	QG	Gr	Gr	OF	OF	N	QG	QG	Gr	N	N	Gr	Gr	ppm
SiO_2	57.32	58.35	55.96	47.91	65.78	67.29	62.06	60.70	55.96	51.01	58.58	58.78	54.90	54.16	69.85	72.96	60
TiO_2	0.54	0.53	0.41	2.35	0.81	0.79	0.43	0.47	0.41	1.50	1.46	0.79	0.28	0.60	0.72	0.57	35
Al_2O_3	16.39	15.97	17.17	11.17	12.77	12.63	9.76	11.43	17.17	13.01	12.62	12.84	18.34	18.03	13.02	12.73	120
Fe_2O_3	8.47	8.86	7.79	16.80	9.43	8.52	8.60	11.47	7.79	14.98	12.90	11.10	6.73	8.32	5.81	2.90	30
MnO	0.15	0.14	0.13	0.19	0.12	0.11	0.31	0.25	0.13	0.18	0.16	0.23	0.12	0.12	0.09	0.04	30
MgO	4.38	5.04	6.43	4.35	1.31	0.90	6.72	4.74	6.43	3.40	2.00	1.72	6.20	4.74	0.45	0.41	95
CaO	8.21	6.56	5.75	9.63	1.81	1.82	5.23	2.93	5.75	8.60	4.90	3.94	8.55	7.74	1.74	2.11	15
Na_2	3.04	3.08	2.48	2.57	2.93	2.93	3.66	3.62	2.48	2.54	2.79	2.92	3.24	3.16	3.71	5.65	75
K_2O	1.47	1.47	1.52	1.19	4.44	4.21	2.40	1.43	1.52	1.63	3.12	3.66	0.77	1.33	3.74	0.99	25
P_2O_5	0.17	0.26	0.12	2.90	0.24	0.23	0.17	0.15	0.12	2.15	1.03	0.40	0.05	0.19	0.13	0.15	35
Ba	621	663	541	663	1295	1446	571	611	632	631	1042	1182	22	58	125	54	15
Ce	56	84	100	170	161	127	60	69	55	150	161	165	25	23	9	10	10
Sc	29	16	16	38	8	9	16	8	18	29	23	15	91	210	11	64	10
V	143	108	78	713	42	87	129	144	391	606	208	130	90	94	102	52	2
Zn	163	128	156	140	285	92	158	137	111	128	161	127	90	94	102	52	2
Ga	19	18	21	20	19	18	10	17	18	21	20	19	19	19	16	12	1
Nb	6	6	6	9	16	11	12	12	12	7	10	9	5	5	13	10	1
Pb	13	13	9	10	18	9	15	18	14	12	18	19	7	6	6	2	1
Rb	46	43	36	39	126	130	55	39	38	73	123	123	23	36	102	34	1
Sr	442	413	471	316	161	190	58	98	368	363	232	231	540	497	191	182	1
Th	12	15	10	17	28	24	11	11	19	17	23	22	5	7	17	7	1
U	5	6	5	8	9	8	8	8	5	8	8	8	4	4	7	5	1
Y	24	27	20	53	44	35	23	22	21	48	47	47	14	20	37	22	1
Zr	195	250	111	158	489	422	126	141	356	182	326	333	31	49	297	149	1
Cl	475	470	98	714	345	389	242	127	265	301	513	532	<LoD	318	180	308	100
F	1077	1518	2003	2932	1629	1687	2163	2858	1307	2761	2759	2754	<LoD	<LoD	<LoD	<LoD	100
S	232	186	137	624	122	6	1397	3645	228	301	15	18	<LoD	<LoD	<LoD	<LoD	100
LOI	0.46	0.73	2.71	0.88	0.46	0.94	0.76	3.04	0.91	1.05	1.27	3.71	1.59	1.61	0.37	0.89	100
Total	100.74	101.10	101.09	100.12	100.27	100.55	100.19	100.33	100.56	100.21	101.00	100.25	100.79	100.04	99.66	99.41	
Qtz	9.35	11.13	8.04	5.47	22.47	25.85	11.42	16.46	10.57	8.05	15.49	14.17	5.23	6.17	28.24	31.58	
C	0.00	0.00	0.00	0.00	0.36	0.43	0.00	0.00	1.26	0.00	0.00	0.00	0.00	0.00	0.02	0.00	
Or	9.58	8.69	7.80	7.03	26.24	24.88	14.19	8.45	8.98	9.63	18.44	21.63	4.55	7.86	2.11	5.85	
Ab	24.45	26.06	26.14	21.74	24.79	24.79	30.97	30.63	20.98	21.49	23.61	24.71	27.41	26.74	31.39	47.80	
An	27.71	24.41	28.90	15.43	7.59	7.72	3.12	10.72	27.80	19.29	12.70	11.12	33.23	31.09	7.78	6.46	
Ne	0.15	0.17	0.10	1.94	0.16	0.15	0.11	0.10	0.08	1.44	0.69	0.27	0.00	0.00	0.00	0.00	
Di	3.38	4.57	9.07	12.76	0.00	0.00	17.73	2.41	0.00	9.01	4.72	5.17	7.10	4.92	0.00	5.54	
Opx	20.45	19.07	14.38	18.69	12.13	10.16	17.08	22.42	23.82	17.62	14.10	12.50	17.25	15.39	4.80	1.23	
Mgt	2.77	3.08	3.22	5.85	3.28	2.96	2.99	3.99	2.71	5.21	4.49	3.86	3.32	4.10	2.86	1.43	
Ilm	0.91	1.01	1.46	4.47	1.53	1.50	0.82	0.89	0.78	2.86	2.78	1.50	0.53	1.14	1.37	1.08	
Ap	0.53	0.62	0.37	6.88	0.56	0.53	0.39	0.36	0.29	5.10	2.44	0.95	0.12	0.45	0.31	0.36	
Total	99.28	98.81	99.48	100.26	99.11	98.97	98.82	96.43	97.27	99.70	99.46	95.88	98.74	97.85	98.88	98.33	

Representative samples of norite (N), quartz gabbro (QG), granophyre (Gr), and Onaping Formation (OF) were analyzed for major and selected trace elements by X-ray fluorescence (XRF) at McGill University. The analyses were done with a Philips PW1400 instrument using fused beads prepared from ignited samples, and an α-coefficient technique. Total iron present has been reported as Fe_2O_3. Oxides are quoted in wt.%, and trace elements, in ppm. <LoD: concentration less than the limit of detection. LOI: loss of ignition. The full dataset is available in Warner (1996).

intrusive complex (Antarctica). Crystals with such a cavity were seen only in separates of subhedral and euhedral apatite, and occur more commonly in norite and quartz gabbro samples than in the granophyre. In some cases, the axial cavity is filled; semiquantitative electron-microprobe analyses show that both orthopyroxene and clinopyroxene are present within the cavity, along with a chlorite-group mineral. The infilling phase(s) may have crystallized from melt trapped during a period of rapid growth of apatite owing to high supersaturation; the chlorite may have formed during devitrification of basic glass.

An examination by cathodoluminescence and a comparison of rim and core compositions (Warner 1996) show that grains are homogeneous and unzoned. Thus in spite of textural evidence for supersaturation, crystal growth was not sufficiently rapid, even in the felsic magma, to lead to concentric or sector zoning. Piccoli & Candela (1994) emphasized that apatite typically crystallizes over a restricted range of temperature, owing to efficient decrease of its solubility due to cooling and to increase in SiO_2 content of the melt. Near-isothermal crystallization would favor unzoned crystals.

CHEMICAL COMPOSITION OF APATITE FROM THE NW SECTION

Selected compositions of apatite from the main mass of the SIC and the overlying Onaping Formation are listed in Table 2; the full dataset is available in Warner (1996). As samples were collected along three traverses (Fig. 2), obvious questions concern not only the differences in apatite composition as a function of height above the base, but also from one traverse to the next. On the basis of petrographic descriptions and previous studies of metamorphic history (*e.g.*, Thomson *et al.* 1985, Fleet *et al.* 1987), one might expect apatite from the NW section to have the most pristine composition.

Substitution in the Ca site

The levels of the *light rare-earth elements (LREE,* ΣLa + Ce + Nd; Fig. 5a) are generally highest in apatite in the Sublayer and norite [up to 18000 ppm or 0.12 atoms per formula unit (*apfu*)], and they decrease in the quartz gabbro (down to 5700 ppm or 0.035 *apfu*). Apatite has similar levels of *LREE* (5500 ppm) from the middle sample of granophyre, then increases slightly in apatite near the top of the granophyre (up to 8300 ppm). In Onaping Formation samples, the levels of *LREE* range from 2300 to 4800 ppm (0.014–0.03 *apfu*). The higher concentration of *LREE* in apatite near the base of the SIC, and systematic decrease toward the granophyre, are opposite of the compositional trends in apatite from the Dufek intrusion (Drinkwater *et al.* 1990), the only one with which a comparison is judged suitable.

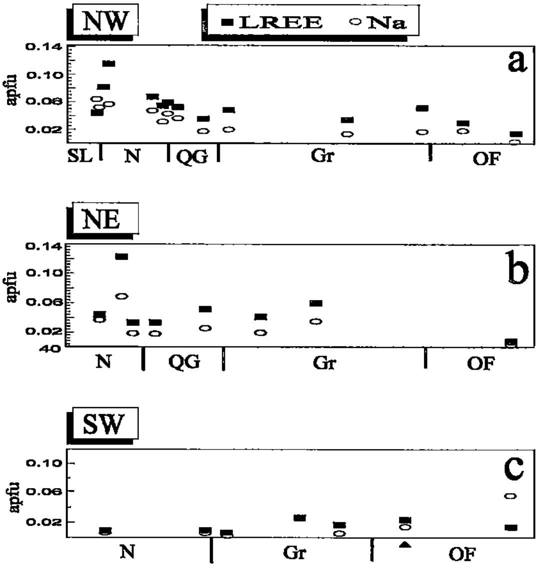

FIG. 5. The concentration of minor elements in apatite from the: a) NW, b) NE, and c) SW sections. SL: Sublayer, N: norite, QG: quartz gabbro, Gr: granophyre, and OF: Onaping Formation. Units are atoms per formula unit, *apfu*. *LREE*: La + Ce + Nd. Stratigraphic height increases toward the right. The scale is the same as in Figure 7.

The apatite separates were analyzed by ICP–MS (solution technique) for their trace-element content, and the results are given in Table 3. Chondrite-normalized patterns of apatite separated from representative samples (Fig. 6a) indicate a consistent distribution of the *REE* in each rock type of the Main Mass; except for the heavy rare-earth elements (*HREE*), the apatite (post-cumulus) from the norite is the most enriched in *REE.* Apatite from the Main Mass has significantly higher levels of *LREE* than of *HREE* ($15 < La_N/Lu_N < 20$), is most enriched in La and Ce, and consistently shows a negative Eu anomaly. The apatite from the NW section is more strongly enriched in *LREE* and, to a lesser extent, the *HREE*, than that from other major tholeiitic complexes.

The concentration of *sodium* in apatite (Fig. 5a) is highest in the Sublayer (up to 2000 ppm or 0.05 *apfu*), decreases systematically with stratigraphic height into the quartz gabbro (<1300 ppm or 0.04 *apfu*), and is 400 ppm in the middle of the granophyre. The levels then increase slightly (to 600 ppm) in the uppermost sample of granophyre. In the Onaping Formation, the levels range from 100 to 600 ppm. Although Na is present in lower concentrations than the *LREE*, its distribution in apatite mirrors that of the *LREE* at all levels of the SIC, as well as in the Onaping Formation. The parallel distribution of Na and the *LREE* is consistent with their incorporation into apatite by a coupled substitution: $2Ca^{2+} = Na^{+} + LREE^{3+}$.

The concentration of *strontium* is lowest in apatite near the base of the complex, in the Sublayer and norite (100–200 ppm or 0.001–0.002 *apfu*; Table 2); it increases in the quartz gabbro and granophyre (500–700 ppm). The levels of Sr in apatite from the Onaping Formation ranges from 100 to 500 ppm. The concentrations of Sr thus increase dramatically within the upper portions of the quartz gabbro and the granophyre, even though Watson & Green (1981) reported that the partitioning of Sr into apatite is insensitive to temperature or melt composition.

The chondrite-normalized distribution pattern of *other trace elements* (Table 3) that substitute for Ca in apatite in five samples from the NW section form a very coherent set (Fig. 6c). In general, the apatite is relatively and uniformly depleted in monovalent cations, which thus behave like Na. The pattern of enrichment of Ba obeys that expected on the basis of well-studied fractionation sequences. Variations in Pb resemble variations in Ba. For the other elements, the samples are all

TABLE 2. SELECTED RESULTS OF ELECTRON-MICROPROBE ANALYSES AND STRUCTURAL FORMULAE OF APATITE IN ROCKS OF THE SUDBURY IGNEOUS COMPLEX AND ONAPING FORMATION

	NW Section									NE Section							SW Section				
Sample	pcl56	pcl53	28	29	45	30	33	36	37	2a	16	4	18	5a	20	10a	64	60	59	56	54
Unit	SL	SL	N	N	QG	QG	Gr	Gr	OF	N	N	QG	QG	Gr	Gr	OF	N	N	Gr	Gr	OF
P_2O_5 wt.%	41.22	40.99	40.77	41.44	40.14	41.09	40.42	41.21	40.47	41.56	40.85	41.61	41.25	40.46	41.38	41.91	41.89	41.97	41.27	41.48	42.43
SiO_2	0.18	0.19	0.44	0.27	0.28	0.11	0.22	0.24	1.09	0.19	0.42	0.12	0.15	0.17	0.27	0.11	0.13	0.07	0.05	0.15	0.35
Al_2O_3	0.00	0.00	0.01	0.11	0.03	n.a.	0.01	0.01	0.41	0.02	0.03	n.a.	0.03	0.04	0.09	0.05	0.11	0.01	0.01	0.01	0.08
FeO	0.12	0.21	0.24	0.43	0.33	n.a.	0.45	0.47	0.45	0.23	0.24	n.a.	0.24	0.42	0.33	0.13	0.08	0.07	0.03	0.14	0.04
MnO	0.07	0.07	0.07	0.04	0.06	n.a.	0.08	0.07	0.04	0.04	0.05	n.a.	0.05	0.05	0.05	0.01	0.07	0.04	0.04	0.02	0.03
MgO	0.04	0.07	0.06	0.06	0.03	n.a.	0.06	0.03	0.46	0.10	0.05	n.a.	0.07	0.04	0.01	0.01	0.00	0.00	0.00	0.00	0.03
CaO	54.71	53.85	53.07	55.97	54.63	54.93	54.63	54.20	52.90	54.78	53.04	55.32	55.23	53.07	53.88	55.92	55.55	55.84	55.50	55.52	55.74
Na_2O	0.16	0.19	0.17	0.10	0.11	0.05	0.04	0.05	0.06	0.11	0.21	0.05	0.08	0.06	0.11	0.01	0.02	0.02	0.01	0.01	0.04
SO_3	0.21	0.12	0.04	0.04	0.01	0.10	0.01	0.01	0.01	0.02	0.02	0.05	0.17	0.01	0.01	0.02	0.05	0.00	0.00	0.01	0.03
SrO	0.02	0.02	0.01	0.00	0.01	0.05	0.07	0.06	0.01	0.04	0.00	0.05	0.02	0.05	0.02	0.02	0.05	0.05	0.02	0.08	0.01
Y_2O_3	0.00	0.02	0.10	0.04	0.01	0.00	0.01	0.02	0.01	0.02	0.03	0.00	0.02	0.02	0.03	0.00	0.01	0.00	0.00	0.00	0.00
La_2O_3	0.13	0.27	0.37	0.17	0.19	0.10	0.10	0.19	0.10	0.13	0.46	0.12	0.11	0.15	0.20	0.02	0.01	0.02	0.01	0.05	0.10
Ce_2O_3	0.42	0.74	0.92	0.48	0.46	0.29	0.29	0.43	0.27	0.38	1.05	0.29	0.38	0.31	0.49	0.09	0.09	0.10	0.04	0.17	0.22
Nd_2O_3	0.16	0.27	0.40	0.21	0.19	0.18	0.16	0.19	0.10	0.18	0.42	0.12	0.33	0.16	0.22	0.01	0.03	0.04	0.04	0.05	0.07
UO_2	0.00	0.00	0.01	0.00	0.01	0.01	0.00	0.01	0.01	0.00	0.00	0.01	0.00	0.03	0.00	0.00	0.00	0.00	0.00	0.01	0.01
ThO_2	0.00	0.00	0.01	0.00	0.00	0.00	0.00	0.00	0.00	0.00	0.00	0.00	0.00	0.01	0.00	0.00	0.01	0.00	0.01	0.00	0.00
F	2.27	2.12	1.99	2.14	2.50	2.85	3.64	3.57	3.34	2.94	3.23	2.53	2.98	3.13	3.79	3.48	2.10	2.72	3.91	3.74	3.01
Cl	1.25	1.31	1.21	0.65	0.81	0.60	0.18	0.14	0.30	0.31	0.22	0.33	0.13	0.05	0.05	0.02	0.62	0.23	0.00	0.01	0.01
Sum	99.72	99.27	99.87	101.09	98.56	100.37	98.80	99.37	98.54	99.74	100.30	100.62	99.95	98.24	100.92	100.34	99.78	99.98	99.29	99.88	100.91
O=F,Cl	1.24	1.19	1.11	1.05	1.24	1.34	1.57	1.54	1.47	1.31	1.41	1.14	1.29	1.33	1.61	1.47	1.02	1.20	1.65	1.58	1.27
Total	98.48	98.08	98.76	100.04	97.33	99.03	97.22	97.84	97.07	98.43	98.89	99.48	98.67	96.91	99.31	98.87	98.75	98.78	97.64	98.30	99.64
Atomic proportions on the basis of (P + Si + S) = 6 atoms and (F + Cl + OH) = 2 atoms																					
P	5.942	5.951	5.919	5.950	5.951	5.968	5.960	5.957	5.814	5.965	5.926	5.973	5.953	5.969	5.953	5.979	5.972	5.987	5.992	5.974	5.939
Si	0.030	0.033	0.076	0.046	0.048	0.019	0.039	0.042	0.185	0.033	0.071	0.020	0.026	0.029	0.045	0.019	0.021	0.012	0.008	0.026	0.058
S	0.027	0.016	0.005	0.005	0.001	0.013	0.001	0.001	0.001	0.002	0.002	0.007	0.021	0.001	0.002	0.002	0.006	0.001	0.000	0.001	0.003
Al	0.001	0.001	0.001	0.022	0.006	0.000	0.003	0.002	0.082	0.004	0.006	0.000	0.005	0.008	0.017	0.010	0.023	0.002	0.002	0.002	0.015
Fe	0.017	0.029	0.034	0.061	0.049	0.000	0.066	0.067	0.064	0.032	0.034	0.000	0.034	0.062	0.046	0.018	0.011	0.009	0.004	0.020	0.005
Mn	0.010	0.010	0.010	0.005	0.009	0.000	0.011	0.010	0.006	0.006	0.007	0.000	0.007	0.008	0.008	0.002	0.010	0.006	0.006	0.002	0.004
Mg	0.009	0.017	0.016	0.014	0.009	0.000	0.016	0.007	0.117	0.024	0.011	0.000	0.017	0.011	0.002	0.002	0.001	0.001	0.000	0.001	0.008
Ca	9.980	9.895	9.753	10.171	10.251	10.095	10.193	9.915	9.619	9.951	9.739	10.050	10.085	9.908	9.810	10.094	10.023	10.080	10.198	10.119	9.874
Na	0.040	0.048	0.043	0.025	0.029	0.013	0.010	0.013	0.014	0.028	0.052	0.014	0.020	0.015	0.026	0.002	0.006	0.004	0.002	0.004	0.010
Sr	0.002	0.002	0.001	0.000	0.001	0.005	0.008	0.006	0.001	0.004	0.000	0.005	0.002	0.005	0.002	0.002	0.005	0.004	0.002	0.008	0.001
Y	0.000	0.002	0.009	0.004	0.001	0.000	0.001	0.002	0.001	0.002	0.003	0.000	0.002	0.002	0.003	0.000	0.001	0.000	0.000	0.000	0.000
La	0.008	0.017	0.023	0.011	0.013	0.006	0.006	0.012	0.006	0.008	0.029	0.008	0.007	0.010	0.013	0.001	0.001	0.001	0.000	0.003	0.006
Ce	0.026	0.047	0.058	0.030	0.030	0.018	0.018	0.027	0.017	0.024	0.066	0.018	0.024	0.020	0.031	0.005	0.005	0.006	0.003	0.010	0.013
Nd	0.010	0.017	0.025	0.013	0.012	0.011	0.010	0.011	0.006	0.011	0.026	0.007	0.020	0.010	0.013	0.001	0.002	0.002	0.003	0.003	0.004
U	0.000	0.000	0.000	0.000	0.000	0.000	0.000	0.000	0.000	0.000	0.000	0.000	0.000	0.001	0.000	0.000	0.000	0.000	0.000	0.000	0.000
Th	0.000	0.000	0.000	0.000	0.000	0.000	0.000	0.000	0.000	0.000	0.000	0.000	0.000	0.000	0.000	0.000	0.000	0.000	0.000	0.000	0.000
F	1.222	1.151	1.078	1.146	1.385	1.546	1.047	1.930	1.791	1.579	1.751	1.357	1.607	1.725	1.087	1.857	1.119	1.448	1.999	1.998	1.574
Cl	0.362	0.380	0.352	0.186	0.241	0.175	0.053	0.040	0.086	0.089	0.065	0.095	0.037	0.016	0.013	0.004	0.176	0.065	0.001	0.002	0.002
OH	0.416	0.469	0.570	0.668	0.375	0.279	0.000	0.030	0.123	0.333	0.183	0.548	0.356	0.259	0.000	0.139	0.705	0.487	0.000	0.000	0.424

Apatite grains were analyzed from samples representing the Sublayer (SL), norite (N), quartz gabbro (QG), granophyre (Gr), and Onaping Formation (OF) with an electron microprobe at McGill University. Concentrations of Ca, P, F, Cl, Si, Al, Fe, Mn, Mg, Na, S, Sr, Y, La, Ce, Nd, U and Th were recorded using wavelength-dispersion spectrometry (JEOL 8900L, accelerating voltage 15 kV, 5-μm beam, and beam current 40 nA). Various synthetic and natural samples (including natural fluorapatite) were used as standards. Counting times for each element varied between 40 and 100 seconds, and halogen loss was minimized by measuring their concentration first. Each composition represents an average result of one core analysis and two rim analyses from one or two grains per polished section. The departures from stoichiometry are judged to be within acceptable limits. All Fe is assumed to be Fe^{2+}. The full dataset is available in Warner (1996).

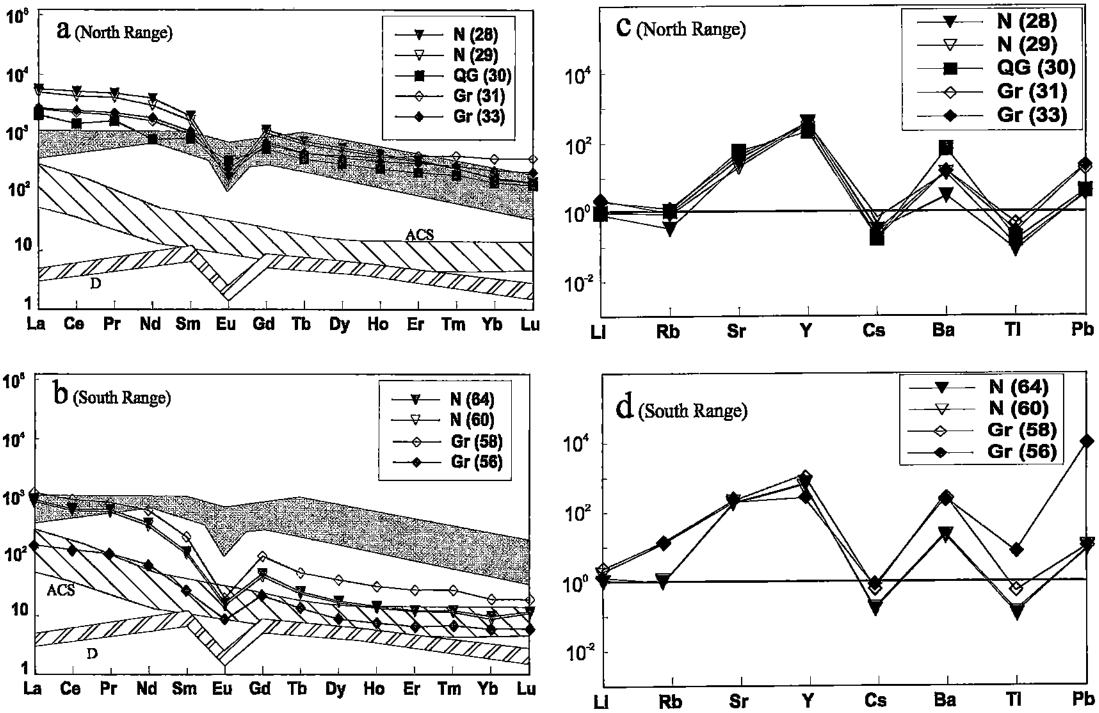

FIG. 6. Chondrite-normalized (apatite/chondrite) *REE* patterns for apatite from the a) NW and b) SW sections. *REE* patterns for apatite from other complexes [Dufek: Drinkwater *et al.* (1990), Skaergaard: Paster *et al.* (1974), and Bjerkrem – Sogndal lopolith: Roelandts & Duchesne (1976)] plot in the shaded area. The *REE* values for the average Canadian Shield (ACS) plot in the band marked by single oblique lines (Shaw *et al.* 1974). Experimentally determined apatite – liquid partition coefficients (*D*) for *REE* (La, Sm, Eu, Dy, Lu) from intermediate to mafic rocks plot in the band marked by doubled oblique lines (Watson & Green 1981). Chondrite-normalized (apatite/chondrite) trace-element patterns for apatite from the c) NW and d) SW section. Legend refers to rock type (sample).

very close; these findings emphasize the close coherence between mafic and felsic portions of this igneous complex.

Substitution in the P site

The levels of *silicon* in apatite are more or less constant across the NW section of the complex (~2000 ppm or 0.03–0.05 *apfu*; Table 2), with the exception of a higher value from a sample of norite (4400 ppm or 0.076 *apfu*) and an anomalously low value from a sample of quartz gabbro (1100 ppm). One sample from the Onaping Formation has levels of Si over 1 wt.% SiO_2 (0.185 *apfu*), but this value may well be suspect, owing to the fineness of the grain size. The other sample from the Onaping Formation has levels of Si in apatite less than 900 ppm (0.015 *apfu*). The high concentration of Si in apatite near the base of the SIC is anomalous compared to other layered complexes, but presumably reflects the coupled substitution with part of the structurally bound *REE*: $Ca^{2+} + P^{5+} = Si^{4+} + REE^{3+}$ (Rønsbo 1989).

The concentrations of *sulfur* are near the detection limit (Table 2); the levels are highest in apatite from the Sublayer (up to 2100 ppm or 0.027 *apfu*), one sample of quartz gabbro (400 ppm or 0.005 *apfu*), and one sample from the Onaping Formation (up to 3400 ppm or 0.043 *apfu*). In every other sample, the apatite contains 100 ppm or less. Naldrett *et al.* (1986) showed that the Sublayer is the site of efficient accumulation of an immiscible sulfide melt unmixed from the overlying silicate melt. Apatite in the Sublayer, therefore, crystallized from a melt whose content of sulfate was relatively low.

Volatile constituents

In general, apatite from the SIC is F-rich (Fig. 7a). The Cl and OH contents decrease from the base of the complex toward the top, whereas apatite in the Onaping Formation has higher inferred levels of OH. The inferred F:Cl:OH proportions of apatite range from 58:18:24 in the Sublayer and norite, to 71:12:17 in the quartz gabbro, 98:2:0 in the granophyre, and 68:3:29 in the Onaping Formation. Although apatite in the SIC shows a steadily increasing level of F with stratigraphic height, as in other layered complexes, that in the Onaping Formation is distinctly enriched in OH.

COMPOSITIONS OF APATITE FROM THE NE AND SW SECTIONS

Many of the same trends are recognized in the composition of apatite from the NE and SW sections (Table 2), along which the rocks are more strongly recrystallized, but there are subtle differences in composition with respect to apatite in the NW section. In all rock types (Fig. 5), the levels of *LREE* in apatite are uniformly lower than those from the NW section. This is especially noticeable near the base of the complex sampled along the SW section, where concentrations are 6 to 12 times lower. Only one sample from the NE section has levels of *LREE* (up to 19000 ppm or 1.24 *apfu*) similar to those expected along the NW section.

Chondrite-normalized patterns show that apatite separated from samples of norite and granophyre from the SW section (Table 3, Fig. 6b) has a conformable *REE* distribution, as in the NW section; apatite from the two samples of granophyre is the most and least enriched in *REE*, whereas that from the samples of norite fall in between. Also as encountered in samples from the NW section, apatite from the SW section has significantly higher levels of *LREE* than of *HREE*, is most enriched in La and Ce, and consistently shows a negative Eu anomaly. The most obvious difference between

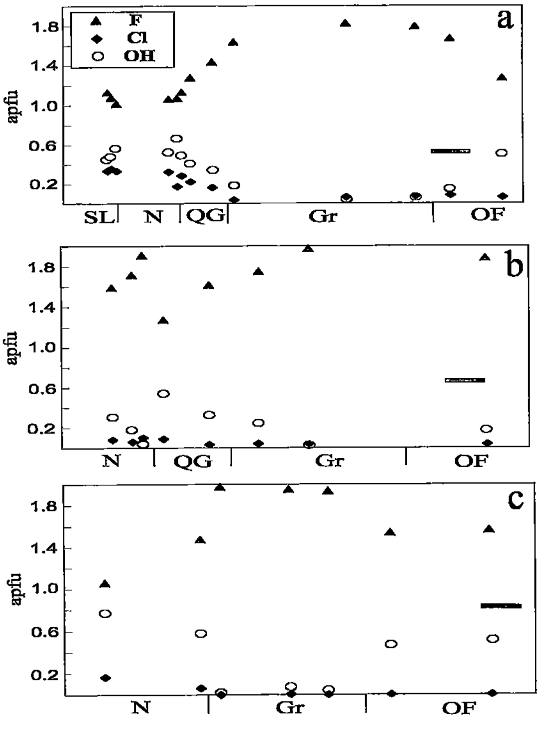

FIG. 7. Volatiles in apatite from the a) NW, b) NE, and c) SW sections. SL: Sublayer, N: norite, QG: quartz gabbro, Gr: granophyre, and OF: Onaping Formation. Units are *apfu*. Bars represent: a) 450 m, b) 400 m, and c) 600 m.

TABLE 3. ICP-MS DATA FOR APATITE FROM THE NW AND SW SECTIONS OF THE SUDBURY IGNEOUS COMPLEX, ONTARIO

	NW Section					LoD	SW Section				LoD
	N	N	QG	Gr	Gr		N	N	Gr	Gr	
	28	29	30	31	33		64	62	58	56	
La	2057	1814	757	946	987	0.002	354	338	417	95	0.002
Ce	4888	4065	1394	2178	2328	0.009	738	711	923	223	0.006
Pr	650	555	225	278	306	0.001	105	99	124	29	0.001
Nd	2794	2115	567	1162	1311	0.021	391	367	533	121	0.015
Sm	456	383	186	220	250	0.019	64	61	92	22	0.009
Eu	15	14	29	18	21	0.006	7.2	6.8	8.0	3.7	0.005
Gd	351	306	165	194	212	0.006	50	47	76	17	0.006
Tb	42	37	21	26	27	0.002	6.2	5.9	9.7	2.3	0.003
Dy	215	193	114	157	145	0.012	33	32	54	13	0.003
Ho	37	35	21	33	28	0.003	6	6	10	3	0.001
Er	87	82	53	101	77	0.010	17	17	28	8	0.004
Tm	9.0	9.0	6.8	14.7	9.9	0.002	2.4	2.4	4.0	1.2	0.002
Yb	40.5	41.9	35.2	91.6	56.5	0.018	15	14	22	8	0.009
Lu	5.3	5.5	4.9	14.1	8.1	0.006	2.5	2.5	3.4	1.1	0.003
Li	2.1	2.4	2.4	5.6	5.1	0.608	1.2	1.4	2.4	1.7	0.497
Rb	1.2	3.1	3.9	3.4	4.5	0.141	1.2	1.2	10.3	9.8	0.038
Sr	312	248	712	431	549	0.808	301	286	336	307	0.23
Y	892	831	484	893	744	0.011	155	147	250	74	0.008
Zr	321	235	18	3365	4365	0.014	2.7	2.4	11.7	24	0.038
Nb	0.2	0.2	0.2	18.6	55.8	0.006	0.2	0.2	0.4	0.4	0.004
Mo	0.4	0.4	0.3	4.2	5.6	0.017	0.3	0.2	13.6	1.7	0.067
Cs	0.1	0.2	0.0	0.1	0.1	0.016	0.0	0.0	0.1	0.1	0.006
Ba	10.4	46.2	241.6	54.4	55.1	0.029	15.0	16.0	125.0	108.0	0.03
Hf	7.9	5.8	0.5	83.2	107.9	0.011	0.1	0.1	0.3	0.2	0.009
Ta	0.0	0.0	0.0	0.8	2.1	0.004	0.0	0.0	0.0	0.0	0.001
Tl	0.0	0.0	0.0	0.1	0.1	0.009	0.0	0.0	0.0	0.4	0.008
Pb	14.3	12.8	15.9	70.5	87.3	0.020	7.6	7.2	8.7	2154	0.079
Bi	0.2	0.0	0.1	1.1	0.3	0.012	0.2	0.3	0.2	12	0.004
Th	24	21	16	390	163	0.002	11	12	31	15	0.007
U	7.8	7.7	4.4	126.4	71.3	0.010	2.2	2.1	15.4	7.1	0.004

Apatite was separated from numbered samples of norite (N), quartz gabbro (QG), and granophyre (Gr) for trace-element analyses. Rock samples were initially crushed to a 0.5-cm grain size with a BICO jaw crusher. Samples were then ground between ceramic plates and sieved. Fractions coarser than 200 mesh were collected for heavy-liquid separation. A Frantz magnetic separator and further heavy-liquid separation removed most grains of mafic minerals, sulfides, and zircon. The apatite was then hand-picked. Samples were analyzed by inductively coupled plasma – mass spectrometry (ICP–MS) using a Sciex Elan model 250 instrument at the Department of Earth Sciences, Memorial University of Newfoundland. Samples were digested in HF and HNO_3, and the solution was analyzed using the method of standard addition to correct for matrix effects (Jenner *et al.* 1990). Concentrations are reported in ppm. The chondrite values of Govindaraju (1989) were used for normalization. LoD: limit of detection.

the *REE* patterns from the NW (Fig. 6a) and SW (Fig. 6b) sections involves the overall concentrations of the *REE*, which are significantly lower (by up to one order of magnitude) in apatite from the SW section.

The concentrations of Na in apatite from the NE section (Fig. 5b) are similar to those reported in the NW section, whereas in the SW section (Fig. 5c), levels of Na (<400 ppm) in apatite from all rock types of the Main Mass are significantly lower. Levels of Na are slightly higher (1700 ppm) in apatite from the Onaping Formation in the SW section. The concentration of Sr in apatite from the NE section (Table 2) is highest near the base of the complex, in the norite (up to 600 ppm) and decreases with stratigraphic height, whereas among samples from the SW section (Table 2), concentrations are highest in the granophyre (up to 800 ppm) and slightly lower in apatite in the norite (<500 ppm). The concentration of Sr in apatite in the Onaping Formation is low in all three sections (<200 ppm).

The concentration of other trace elements that substitute for Ca in apatite from the SW section (Fig. 6d) is similar to that from the NW section (Fig. 6c), but the samples do not form as coherent a set; especially variable in apatite from the SW section are Pb, Tl, Ba, and Rb. In general, apatite from samples of granophyre is the most enriched in these trace elements.

The concentration of Si in apatite from the NE section (Table 2) is similar to that from the NW section (~2000 ppm), whereas levels of Si from the SW section are less than 1500 ppm in all rock types of the Main Mass, and slightly higher in the Onaping Formation. Just as in the NW section, the levels of sulfur from the NE and SW sections are low in every rock type (<500 ppm), with the exception of higher values in the quartz gabbro (1700 ppm) from the NE section (Table 2).

Concentrations of the volatile components found in apatite are slightly more variable in the NE and SW sections (compared to the NW section), with lower levels of Cl and more irregular concentrations of F. In the NE section (Fig. 7b), inferred F:Cl:OH proportions range from approximately 85:5:10 in the norite and quartz gabbro, up to 96:4:0 in the granophyre, and 90:2:8 in the Onaping Formation. In the SW section (Fig. 7c), the proportion ranges from 65:5:30 at the base of the complex, 97:1:2 in the granophyre, and 80:4:20 in the Onaping Formation. In general, levels of Cl near the base of the complex from the NE and SW sections are up to six times lower than those reported from the NW section. To a large extent, these differences are attributed to the metamorphic overprint (see below).

Unit-Cell Dimensions

Unit-cell parameters are listed in Table 4 for apatite separates from samples of Sublayer, norite, quartz gabbro, and granophyre on the North and South ranges. As expected, because the apatite in all samples from the SIC is relatively F-rich, their cell dimensions plot close to those of fluorapatite (Warner 1996). Samples of F-rich apatite in the granophyre from either limb of the SIC have dimensions closest to those of end-member fluorapatite. Apatite in the norite and Sublayer from the NW section, which have the highest concentration of Cl and *LREE* (*cf.* Fig. 5), plot toward the chlorapatite end-member, which has a larger *a* and smaller *c* dimension (Hughes *et al.* 1989).

The levels of incorporation of the *REE* in apatite from the SIC are similar to those in the samples of *REE*-bearing fluorapatite studied by Hughes *et al.* (1991) having the lowest concentration of *REE*. Apatite from the SIC has a shorter *c* dimension than all of the synthetic *REE*-doped fluorapatite (Fleet & Pan 1995), suggesting that it is substitution in the anionic site that is the more important variable in determining the unit-cell dimensions of apatite.

The volume of the apatite unit-cell (Table 4) is expected to increase with increasing levels of *LREE*-for-Ca(2) and Cl-for-F substitution (Hughes *et al.* 1989, 1991). The apatite samples from the SIC with the highest levels of Cl and *LREE* (*e.g.*, those from the norite and Sublayer) do indeed have the largest volume, whereas the apatite samples that are F-rich and depleted in *LREE* (*e.g.*, those from the granophyre) have the smallest volumes observed. Note that the unit-cell volume of the apatite in the granophyre, as that from the Kiglapait intrusive complex, the only one for which such data are reported (Huntington 1979), is smaller than the unit-cell volume cited for end-member fluorapatite.

^{87}Sr/^{86}Sr Ratio of the Apatite

If apatite is as inert as it is reputed to be (*e.g.*, Creaser & Grey 1992), it would seem to be an excellent monitor of the ^{87}Sr/^{86}Sr value of the magma at the time of

TABLE 4. UNIT-CELL DIMENSIONS OF APATITE FROM THE SUDBURY IGNEOUS COMPLEX

Specimen	*a* (Å)	*c* (Å)	*V* (Å^3)
North Range			
Granophyre 32	9.3823(07)	6.8796(09)	524.46(08)
Quartz Gabbro 30	9.4037(08)	6.8719(09)	526.27(09)
Norite 29	9.4282(08)	6.8718(07)	529.01(09)
Norite 28	9.4247(14)	6.8684(11)	528.36(14)
Sublayer Pcl-53-56	9.4099(17)	6.8762(13)	527.29(17)
South Range			
Granophyre 58	9.3738(11)	6.8839(09)	523.84(11)
Norite 64	9.4144(06)	6.8772(08)	527.87(03)
Norite 62	9.3895(05)	6.8829(07)	525.52(06)

A powder X-ray-diffraction pattern was recorded of apatite separates using a Guinier – Hägg focussing camera (Cu$K\alpha_1$ radiation, synthetic spinel added as an internal standard, *a* equal to 8.0833 Å at room temperature). The cell parameters were refined using the program of Appleman & Evans (1973), as modified by Garvey (1986), and indexed, corrected peaks. The number in brackets is the error in the last two decimal places. The technique of sample separation is as described in Table 3.

growth. The $^{87}Sr/^{86}Sr$ values determined on hand-picked concentrates of apatite are given in Table 5. Apatite in rocks from the North Range (Fig. 8) has consistent values of $^{87}Sr/^{86}Sr$ for each of the principal rock-types of the Main Mass; values range from 0.7072 to 0.7087. On the South Range, values are somewhat higher and more variable over the same stratigraphic interval; apatite from the norite exhibits values of 0.7087 and 0.7098, whereas for the granophyre, the values are 0.7133 and 0.7396. As the apatite contains very little Rb (Figs. 6c, d), the isotopic ratio measured today is virtually identical to its value at the time of emplacement, unless, of course, open-system behavior involving mobilization of ^{87}Sr has affected the apatite.

COMPOSITION OF APATITE NEAR MICROFRACTURES

Electron-microprobe traverses across microfractures in apatite from the NW, NE, and SW sections (Warner 1996, Table 5) were carried out to test whether the compositional differences attributed to the metamorphic overprint are due to changes that occurred along cracks. Apatite grains were selected from norite samples from each section because these have high concentrations of Cl, *LREE*, and Na. In general, in samples 17 (NE section), 26 (NW) (Fig. 9), and 64-1 (SW) (not shown), the concentrations of Cl, *LREE*, Na, and P tend to decrease across the fractures, whereas that of Si increases. Sample 64-2 (SW; not shown) shows similar results, except that Si and *LREE* both increase significantly at one point as a result of an inclusion of allanite (<30 μm across). Allanite is commonly found along fractures in apatite in rocks along the South Range, whereas none was found in the North Range.

In view of the modifications documented in Figure 9, it is reasonable to attribute part of the reduced levels of Cl in apatite from the SW and NE sections to chemical modification along fractures during a metamorphic event. Distinctly lower levels of *LREE*, Na, Si in apatite from the SW section suggest that they are leached in a

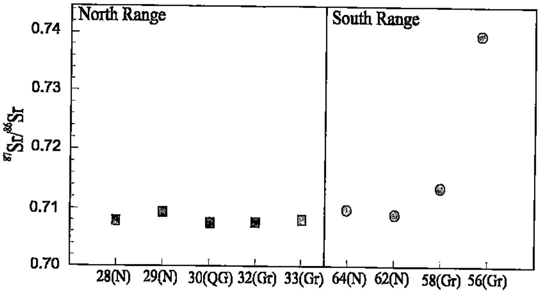

FIG. 8. Strontium isotopes in apatite from the SIC on the North and South ranges. Samples are shown with the rock type in brackets. The standard error associated with these values is smaller than the size of the symbols.

TABLE 5. $^{87}Sr/^{86}Sr$ IN APATITE FROM THE SUDBURY IGNEOUS COMPLEX

Specimen	$^{87}Sr/^{86}Sr$	Specimen	$^{87}Sr/^{86}Sr$
North Range		South Range	
Granophyre 33	0.70746(21)	Granophyre 56	0.73960(15)
Granophyre 32	0.70727(04)	Granophyre 58	0.71326(07)
Quartz Gabbro 30	0.70721(01)	Norite 62	0.70871(04)
Norite 29	0.70873(04)	Norite 64	0.70975(28)
Norite 28	0.70785(05)		

The apatite separates from norite, quartz gabbro and granophyre were analyzed with a VG Sector multi-colector mass spectrometer at the Université du Québec à Montréal. The number in brackets is the error in the last two decimal places. The ratio $^{87}Sr/^{86}Sr$ in standard NBS981 was found to be 0.71024. The technique of mineral separation is as described in Table 3.

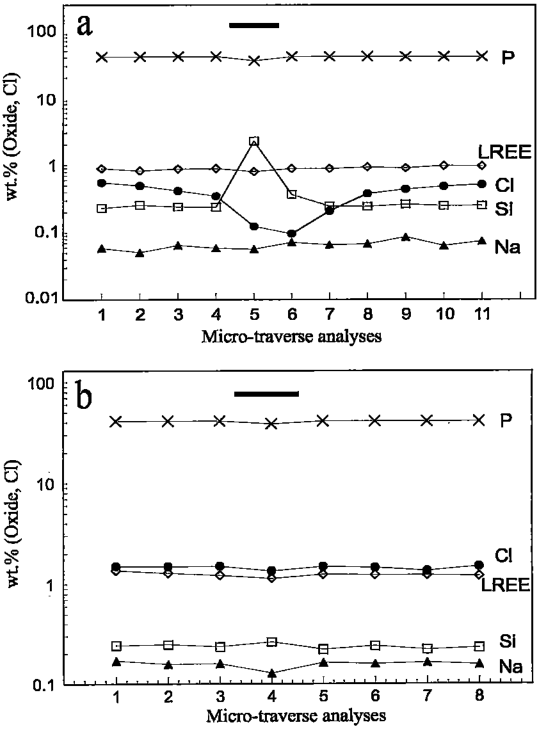

FIG. 9. Electron-microprobe traverses across fractures in apatite from norite samples: a) sample 17 (NE section) and b) sample 26 (NW section). Bar in each diagram represents the position of an apatite fracture. Distance between each point in a) is 5 μm, and in b), 7 μm. Units are wt.%, and the scale is logarithmic. *LREE*: (La_2O_3 + Ce_2O_3 + Nd_2O_3.

coupled fashion, a consequence of their coupling in the structure, as described by Lieftink *et al.* (1994) in apatite from Ødegårdens Verk (Norway). However, the lack of a dense network of fractures in the apatite from the SW section, and the absence of striking modifications in back-scattered electron images of such grains, suggest that the modifications along fractures are of minor consequence.

DISCUSSION

Stratigraphic trends

An examination of the primary, magmatic compositions of apatite is best accomplished with samples from the NW section, which are considered the least disturbed. In theory, the compositional trends are controlled by the sequence of crystallization and the partition coefficients (*D*) of elements that substitute into apatite and the coexisting minerals crystallizing from the evolving magma. Post-cumulus apatite near the base of the complex crystallized from an intercumulus liquid, whereas cumulus and intergranular apatite from the quartz gabbro and granophyre, respectively, crystallized from a late-stage fractionated liquid. According to Green (1994), both plagioclase and orthopyroxene have D_{LREE} less than 1 with respect to a melt, whereas apatite has a D_{LREE} much greater than 1, *i.e.*, apatite is the primary mineral most likely to host the *LREE* in this suite. The *LREE* are thus expected to partition into the intercumulus melt rather than in the cumulus silicate minerals. As the intercumulus liquid becomes enriched in *LREE*, local concentration should be reflected in the post-cumulus apatite. The concentration of the *LREE* in apatite is, in fact, highest in samples from the norite and Sublayer (*cf.* Fig. 6), which crystallized before the melt had apatite on the liquidus. Saturation of apatite is expected to occur nearer the liquidus as the melt becomes more silicic owing to fractional crystallization (Watson 1980). Such saturation occurred in the quartz gabbro (Table 1), close to the point of saturation of the magma in magnetite and ilmenite (Naldrett & Hewins 1984), as is typical of a fractionating tholeiitic liquid. The concentration of *LREE* in apatite then drops in samples of granophyre (Fig. 5a), which crystallized from a melt that presumably had become depleted in *LREE* as a result of apatite saturation and removal from the system. The enrichment in *REE* near the base of the SIC is anomalous, in comparison to other stratiform complexes, and is considered to be related to the high proportion of a crustal contaminant even in the least evolved units of the complex.

Hughes *et al.* (1991) have proposed that the typical *REE* pattern for apatite should be concave downward centered on Nd, in view of ionic radius and bond-valence requirements. Presumably for these reasons, D_{MREE} values are higher than D_{LREE} or D_{HREE} for apatite, according to Green (1994) and Watson & Green (1981). The apatite from the SIC departs from the predicted profile in being more enriched in *LREE* than in *MREE* (Fig. 6a), as are bulk rocks of the SIC (Naldrett & Hewins 1984), and the potential crustal component of the SIC, modeled here by the average profile of the Canadian Shield (Shaw *et al.* 1974). The *REE* budget of the apatite from the SIC is controlled by the bulk composition of the evolving magma, which seems strongly influenced by its crustal contaminant, such that the growing apatite, the only phase to significantly host the *REE*, simply accepted the populations of *REE* as available in the melt. Partition coefficients imply equilibrium growth; in the case of the *REE*, these possibly were violated owing to rapid crystallization of the entire complex.

Apatite from the Onaping Formation is sparse, and its ultimate origin (*i.e.*, xenocrystic or crystallized from an impact-generated melt) is still not established. It has broadly similar trends to that in the granophyre; it is F-rich, LREE- and Na-poor, and the levels of Si and S are comparable to those reported in samples of the underlying granophyre. Conversely, the differences are judged to be indication of a more complex petrogenetic history for rocks of Onaping Formation; the higher inferred levels of OH in apatite, in particular, are consistent with formation from a magma that was in the process of violent degassing upon emplacement.

Comparison with other layered complexes

The apatite from the Sudbury igneous complex has a vertical distribution generally comparable to what has been documented in other subalkaline layered igneous complexes. Typically, the modal proportion of post-cumulus apatite near their base is less than 1 vol.%, like at Sudbury. The proportion of cumulus apatite, in contrast, may reach up to 10 vol.% (Kiglapait: Huntington 1979), or even 30 vol.% (Bushveld: Cawthorn & Walsh 1988, Boudreau & Kruger 1990) (7 vol.% in the SIC). The characteristics of apatite from capping granophyres have only been documented in the Dufek intrusion; the modal concentrations of apatite there (up to 1.2 vol.%: Drinkwater *et al.* 1990) also are comparable to those in granophyric rocks in the SIC.

As in the case of the SIC (Fig. 7), fluorapatite is the typical apatite-group mineral of other layered igneous complexes, with the notable exception of the ultramafic sequences at the base of the Bushveld and Stillwater intrusions, which contain chlorapatite (over 7 wt.% Cl). Above such zones of the Bushveld and Stillwater complexes, and in compositions reported from each of the other layered complexes, the fluorapatite exhibits a crudely systematic decrease in the level of Cl upsection. Cumulus apatite, which is reported in the Skaergaard (Nash 1976), Kiglapait, Bushveld, and Dufek intrusions, contains the highest levels of F in general.

The concentration of *LREE* (up to 2 wt.% *LREE*$_2$O$_3$) in apatite from the SIC (Fig. 5) is at least twice as high as that reported in any other tholeiitic complex, except for chlorapatite from the lower sequences of the Stillwater Complex (also up to 2 wt.%: Boudreau & McCallum 1989, Meurer & Boudreau 1996). On the other hand, the level of *HREE* in apatite from the SIC is only slightly higher than that reported for the Dufek, Skaergaard, and Bjerkrem – Sogndal (Roelandts & Duchesne 1979) complexes (Fig. 6a). Differences with other complexes can be attributed to the anomalously high *LREE*/*HREE* ratio in the SIC magma (Naldrett & Hewins 1984). At the base of the Bushveld, Stillwater, and Munni Munni (Boudreau *et al.* 1993) layered complexes, the relatively Cl-rich post-cumulus apatite has the highest concentration of *LREE*, whereas cumulus apatite has the lowest levels. A notable exception is apatite from the Skaergaard intrusion (Nash 1976), which apparently shows no variation in levels of *LREE* with stratigraphic height. Also, unlike the SIC, the levels of *LREE* in apatite from Dufek are higher in apatite from the capping granophyre than in that from the lower units. This difference reflects the fact that the SIC magma, even at the deepest parts of the sections sampled, is significantly more *LREE*-rich than the parental magma in other stratiform igneous complexes.

Variations in proportions of the volatile constituents

Pristine apatite from the SIC invariably is close to end-member fluorapatite (Fig. 7). Levels of Cl and OH are highest in apatite near the base of the SIC and decrease up-section. As anhydrous phases such as plagioclase and orthopyroxene crystallized in vast quantities, the residual melt increasingly approached saturation in a volatile phase. Once bubbles nucleated, it is reasonable to propose that they coalesced and began to rise. The marked drop in Cl (and inferred for OH) in pristine apatite from the SIC can be attributed to progressive degassing of the melt well before apatite became a cumulus phase, and to decreasing temperature (Piccoli & Candela 1994). Escape of a volatile fluid phase from a vapor-saturated magma is expected to cause a decrease in Cl relative to F, because Cl shows a strong preference for an orthomagmatic fluid phase, and F is more likely to remain in a silicate melt (Candela 1986). In the presence of a melt or magmatic volatile phase, apatite will preferentially exclude Cl^- because of its much larger ionic radius than F^- or OH^- (r = 1.7 Å *versus* 1.4 Å: Shannon 1976). Halogen concentrations found in apatite will reflect the relative proportions of F and Cl in the residual melt upon crystallization of apatite. The F-dominant composition of cumulus and intergranular apatite in the quartz gabbro and granophyre, respectively, is taken to reflect the composition of the bulk magma after Cl and H$_2$O have already commenced to escape.

A comparison of apatite on the North and South ranges

On the basis of an assumption that the entire lopolithic igneous complex, whatever its origin, formed at one point in time, what is formed along the northern and southern sides of the structure should be very similar, if one allows for regional differences in the nature of the crustal contaminant. If one accepts this assumption, the compositional differences noted between the more pristine NW section and the more strongly recrystallized NE and SW sections may be explained in terms of a regional metamorphic overprint, the influence of which waned northward. Rocks on the North Range have been metamorphosed to the greenschist facies only, and those on the South and East ranges, locally up to the amphibolite facies (Thomson *et al.* 1985, Fleet *et al.* 1987). Grains of apatite in rocks along the South Range are smaller, less plentiful, and more intensely fractured than those on the North Range; these features are attributed to brittle deformation and comminution during the northwesterly directed thrusting of the South Range.

Tacker & Stormer (1989) determined experimentally that apatite is relatively immune to low-temperature re-equilibration by diffusive processes, and high-temperature (>500°C) hydrothermal dissolution also is not significant in changing the compositions of apatite. On the other hand, apatite – fluid interaction is known empirically to affect the composition of apatite. Lieftink *et al.* (1994) determined that with increasing metamorphic temperatures, Cl in chlorapatite from Ødegårdens Verk (Norway) is replaced by OH or F along reaction fronts along cracks in the grains. Similar alteration has been described in low-temperature environments. Boudreau & McCallum (1990) described the leaching of chlorapatite and increased mobility of the *REE* in the Stillwater Complex as a result of deuteric alteration. In each case, halogen re-equilibration occurred by recrystallization in the presence of a fluid.

Apatite from the NE and SW sections has significantly lower levels of Cl, *LREE*, Si, and Na than the apatite from the NW section. Traverses across microfractures in apatite (Fig. 9) suggest that concentrations of Cl, Na, and P decrease locally only. The loss of Cl near fractures indicates that Cl was leached from apatite in the presence of a pore fluid. Because of significantly higher metamorphic temperatures on the South Range, we contend that the composition and morphology of apatite were modified through dissolution to a greater degree than in rocks on the North Range. The overall lower concentrations of Cl, *LREE*, Na, and Si in apatite from the SW section are attributed to reactions affecting entire grains, rather than to changes along discrete microfractures.

The close spatial association of allanite found in small and fractured grains of apatite from the South

Range implies that the allanite also results from a metamorphic reaction involving the apatite. On the basis of these findings and the increase in $^{87}Sr/^{86}Sr$ (see below), it seems likely that entire grains were "processed" as a result of metamorphic recrystallization on the South Range.

Variations in the $^{87}Sr/^{86}Sr$ ratio of apatite

Whole-rock $^{87}Sr/^{86}Sr$ values for the SIC, determined from individual rock samples, using an assumed age on both the North and South ranges (Gibbins & McNutt 1975), and for North Range rocks only (Hurst & Farhat 1977), are in the range of 0.706–0.707 for the norite, and 0.700 to 0.711 for the granophyre. The initial ratio determined from isochron plots is approximately 0.707. Apatite in rocks from the North Range (Fig. 8) has conformable $^{87}Sr/^{86}Sr$ values for each of the principal rock-types of the Main Mass. Therefore, the $^{87}Sr/^{86}Sr$ ratio in apatite from the SIC, like the plots of conformable chondrite-normalized distribution of trace elements, suggest that the granophyre is a product of crystal fractionation from a single parental basic magma.

The somewhat higher values in apatite from the South Range (*cf.* Table 5) are most likely the result of homogenization of the $^{87}Sr/^{86}Sr$ ratio during metamorphism to the lower amphibolite grade (Thomson *et al.* 1985), at which grade isotopic homogenization, at least on an intramineral scale, is extremely likely (Faure 1986). Rubidium-rich minerals, such as alkali feldspar, generate locally high concentrations of ^{87}Sr, which are expected to exchange with the strontium of the rubidium-free apatite *via* a pore fluid generated during prograde metamorphic recrystallization. This effect is much more pronounced for apatite from granophyric rocks (Table 5) simply because these contain much more K-feldspar, and thus Rb, than the basic rocks.

Origin of the Sudbury Structure

The consensus today is that the Sudbury Structure formed by impact (Deutsch 1994), but magma sources for the SIC have yet to be firmly established. Three hypotheses are still being evaluated: (1) the magma formed by melting of the upper and lower crust as a result of a meteor impact (Faggart & Basu 1985, Grieve 1991, Dickin *et al.* 1992, Deutsch 1994, Stöffler *et al.* 1994); (2) the impact crater was filled with mantle-generated magma, which assimilated and mixed with shock-melted crustal rocks (Kuo & Crocket 1979, Naldrett *et al.* 1986, Walker *et al.* 1991), and (3) a meteor impact melted crustal rocks, producing the granophyre-forming magma, whereas the basic liquid that crystallized as the norite and quartz gabbro was a mantle-derived melt that rose into the newly formed crater (Chai & Eckstrand 1993, 1994).

The ultimate origin of the Sudbury Structure cannot be determined solely by examining apatite, but the chemical and isotopic properties of apatite from the NW section do point to the likely hypothesis. Apatite in the lower cumulates of the SIC exhibits a crystallization history that is comparable to that in other stratiform igneous complexes. In the Dufek (Drinkwater *et al.* 1990) and other classical stratiform igneous complexes, the granophyre is considered to be the result of a combination of crystal fractionation and anatectic reactions along the contact between crustal rocks and mantle-derived melt. In such a case, the chemical composition of the resultant complex of rocks, in particular the isotopic composition, can be expected to be bimodal, with apatite from the granophyre and lower cumulates giving distinct signatures. This is not the case for apatite from the SIC. The chondrite-normalized *REE* patterns and the $^{87}Sr/^{86}Sr$ ratios (0.707–0.708) in apatite from each unit of the Main Mass from the North Range are very consistent. These trends signify that the SIC (at least the Main Mass) evolved normally by fractional crystallization of a single batch of relatively homogeneous but highly contaminated or crust-derived basic magma. The relatively high initial $^{87}Sr/^{86}Sr$ values and *LREE* enrichment also signify that the basic magma cannot be derived from partial melting of a normal mantle source. Details about the apatite suggest that the impact crater was filled with a single batch of magma formed by melting of the Archean and Early Proterozoic crustal rocks comminuted by the meteor impact. Further evaluations of the source of the magma clearly will require thorough geochemical and isotopic characterization of the basement near the Sudbury Structure.

CONCLUSIONS

1. Apatite from the NW section occurs as a post-cumulus phase near the base of the SIC; it becomes a cumulus phase in the quartz gabbro and an intergranular mineral in the granophyre. Rim and core analyses, cathodoluminescence, and $^{87}Sr/^{86}Sr$ values indicate that the primary apatite is homogeneous, despite the presence of textural signs of rapid growth.
2. The composition of apatite evolves up-section by systematic changes in the proportions of F:Cl:OH and many of the minor elements, from *LREE*-rich and relatively Cl-rich post-cumulus apatite to *LREE*-poor and F-rich cumulus and intergranular apatite. Decrease in OH and Cl are interpreted to accompany degassing of the magma.
3. The chondrite-normalized trace-element patterns and $^{87}Sr/^{86}Sr$ values are consistent and concordant in the relatively unmetamorphosed apatite from each rock type of the Main Mass. The high initial $^{87}Sr/^{86}Sr$ values (>0.707) in apatite indicate that the relatively silica-rich basic magma had a substantial crustal component or possibly consisted entirely of remelted lower crust. Ultimately, the apatite from the norite and that from the granophyre must have had a common magmatic source, suggesting that the complex evolved by fractionation

from a single batch of relatively basic though highly contaminated magma.

4. The compositional and textural features of apatite from the SW section, and to a lesser extent, the NE section, are the result of fluid-mediated adjustments to the composition and morphology of apatite during at least one metamorphic event. Deformation also was a contributing factor. Relative to apatite from the NW section, that from the SW section is consistently depleted in Cl, *LREE*, Na, and Si.

5. Metamorphism on the South Range has reset ^{87}Sr/^{86}Sr values in the apatite in a homogeneous fashion, which suggests a solution-and-redeposition process. If apatite, a relatively inert mineral, has been dissolved and reprecipitated in modified form, then all the other rock-forming minerals likely have re-equilibrated as well.

6. Rocks of the Sudbury Igneous Complex offer a unique opportunity to document the effects of metamorphic recrystallization in a steep regional gradient.

ACKNOWLEDGEMENTS

We appreciate the technical assistance of Glenn Poirier (McGill) with the electron-microprobe analyses, Dr. Simon Jackson, formerly of the Memorial University of Newfoundland, with induced coupled plasma – mass spectrometry, and Glenna Keating and Tariq Ahmedali (McGill) with X-ray fluorescence analyses. We thank P. Lightfoot, then at the Ontario Geological Survey, for providing the samples of Sublayer. We acknowledge the helpful reviews provided by Drs. P.A. Candela, D. London and Associate Editor John M. Hughes, who handled this manuscript.

REFERENCES

APPLEMAN, D.E. & EVANS, H.T., JR. (1973): Job 9214: Indexing and least-squares refinement of powder diffraction data. *U.S. Geol. Surv., Comput. Contrib.* **20** (*NTIS Document* **PB2-16188**).

BETHUNE, K.M. & DAVIDSON, A. (1997): Grenvillian metamorphism of the Sudbury diabase dyke-swarm, Ontario: from protolith to two-pyroxene – garnet coronite. *Can. Mineral.* **35**, in press.

BICKFORD, M.E., VAN SCHMUS, W.R. & ZIETZ, I. (1986): Proterozoic history of the midcontinent region of North America. *Geology* **14**, 492-496.

BOUDREAU, A.E. & KRUGER, F.J. (1990): Variation in the composition of apatite through the Merensky Cyclic Unit in the Western Bushveld Complex. *Econ. Geol.* **85**, 737-745.

________, LOVE, C. & HOATSON, D.M. (1993): Variation in the composition of apatite in the Munni Munni Complex and associated intrusions of the West Pilbara Block, Western Australia. *Geochim. Cosmochim. Acta* **57**, 4467-4477.

________ & MCCALLUM, I.S. (1989): Investigations of the Stillwater Complex. V. Apatites as indicators of evolving fluid composition. *Contrib. Mineral. Petrol.* **102**, 138-153.

________ & ________ (1990): Low temperature alteration of REE-rich chlorapatite from the Stillwater Complex, Montana. *Am. Mineral.* **75**, 687-693.

CANDELA, P.A. (1986): Toward a thermodynamic model for the halogens in magmatic systems: an application to melt – vapour – apatite equilibria. *Chem. Geol.* **57**, 289-301.

CAWTHORN, R.G. & WALSH, K.L. (1988): The use of phosphorus content in yielding estimates of the proportion of trapped liquid in cumulates of the Upper Zone of the Bushveld Complex. *Mineral. Mag.* **52**, 81-89.

CHAI, GANG & ECKSTRAND, R. (1993): The Sudbury Igneous Complex – differentiate of two separate magmas. *Geol. Surv. Can., Pap.* **93-1E**, 219-230.

________ & ________ (1994): Rare-earth element characteristics and the origin of the Sudbury Igneous Complex, Ontario, Canada. *Chem. Geol.* **113**, 221-244.

CREASER, R.A. & GRAY, C.M. (1992): Preserved initial ^{87}Sr/^{86}Sr in apatite from altered felsic igneous rocks; a case study from the middle Proterozoic of South Australia. *Geochim. Cosmochim. Acta* **56**, 2789-2795.

DEUTSCH, A. (1994): Isotope systematics support the impact origin of the Sudbury Structure (Ontario, Canada). *Geol. Soc. Am., Spec. Pap.* **293**, 289-303.

________ & GRIEVE, R.A.F. (1994): The Sudbury Structure: constraints on its genesis from Lithoprobe results. *Geophys. Res. Lett.* **21**, 963-966.

DICKIN, A.P., RICHARDSON, J.M., CROCKET, J.H., MCNUTT, R.H. & PEREDERY, W.V. (1992): Osmium isotope evidence for a crustal origin of platinum group elements in the Sudbury nickel ore, Ontario, Canada. *Geochim. Cosmochim. Acta* **56**, 3531-3537.

DRESSLER, B.O., GUPTA, V.K. & MUIR, T.L. (1984): The Sudbury Structure. *In* Geology of Ontario. *Ont. Geol. Surv., Spec. Vol.* **4**, 593-625.

________, WEISER, T. & BROCKMEYER, P. (1996): Recrystallized impact glasses of the Onaping Formation and the Sudbury Igneous Complaex, Sudbury Structure, Ontario, Canada. *Geochim. Cosmochim. Acta* **60**, 2019-2036.

DRINKWATER, J.L., CZAMANSKE, G.K. & FORD, A.B. (1990): Apatite of the Dufek intrusion: distribution, paragenesis, and chemistry. *Can. Mineral.* **28**, 835-854.

FAGGART, B.E., JR. & BASU, A.R. (1985): Origin of the Sudbury Complex by meteoritic impact: neodymium isotopic evidence. *Science* **230**, 436-439.

FAURE, G. (1986): *Principles of Isotope Geology*. Wiley, New York, N.Y.

FLEET, M.E., BARNETT, R.L. & MORRIS, W.A. (1987): Prograde metamorphism of the Sudbury Igneous Complex. *Can. Mineral.* **25**, 499-514.

________ & PAN, YUANMING (1995): Site preference of rare earth elements in fluorapatite. *Am. Mineral.* **80**, 329-335.

GARVEY, R. (1986): LSUCRIPC, least-squares unit cell refinement with indexing on the personal computer. *Powder Diffraction* **1**, 114.

GIBBINS, S.F.M., GIBSON, H.L. & JONASSON, I.R. (1996): The Onaping Formation: a product of passive and explosive hydroclastic fragmentation of an impact melt? *Geol. Assoc. Can. – Mineral. Assoc. Can., Program Abstr.* **21**, 35.

GIBBINS, W.A. & MCNUTT, R.H. (1975): The age of the Sudbury Nickel Irruptive and Murray pluton. *Can. J. Earth Sci.* **12**, 1970-1989.

GOVINDARAJU, K. (1989): 1989 compilation of working values and sample description for 272 geostandards. *Geostandards Newsletter* **13** (special issue), 1-113.

GREEN, T.H. (1994): Experimental studies of trace-element partitioning applicable to igneous petrogenesis – Sedona 16 years later. *Chem. Geol.* **117**, 1-36.

GRIEVE, R.A.F. (1991): The Sudbury Structure: controversial or misunderstood? *J. Geophys. Res.* **96**, 22753-22764.

HUGHES, J.M., CAMERON, M. & CROWLEY, K.D. (1989): Structural variations in natural F, OH, and Cl apatites. *Am. Mineral.* **74**, 870-876.

________, ________ & MARIANO, A.N. (1991): Rare-earth ordering and structural variations in natural rare-earth-bearing apatites. *Am. Mineral.* **76**, 1165-1173.

HUNTINGTON, H.P. (1979): Kiglapait mineralogy. I. Apatite, biotite, and volatiles. *J. Petrol.* **20**, 625- 652.

HURST, B.W. & FARHAT, J. (1977): Geochronological investigations of the Sudbury Nickel Irruptive and the Superior Province granites north of Sudbury. *Geochim. Cosmochim. Acta* **41**, 1803-1815.

JENNER, G.A., LONGERICH, H.P., JACKSON, S.E. & FRYER, B.J. (1990): ICP–MS – a powerful tool for high precision trace element analysis in earth sciences; evidence from analysis of selected USGS reference samples. *Chem. Geol.* **83**, 133-148.

KROGH, T.E., DAVIS, D.W. & CORFU, F. (1984): Precise U–Pb zircon and baddeleyite ages for the Sudbury area. *In* The Geology and Ore Deposits of the Sudbury Structure. *Ont. Geol. Surv., Spec. Vol.* **1**, 431-446.

KUO, H.Y. & CROCKET, J.H. (1979): Rare earth elements in the Sudbury Nickel Irruptive: comparison with layered gabbros and implications for Nickel Irruptive petrogenesis. *Econ. Geol.* **74**, 590-605.

LIEFTINK, D.J., NIJLAND, T.G. & MAIJER, C. (1994): The behavior of rare-earth elements in high temperature Cl-bearing aqueous fluids: results from the Ødegårdens Verk natural laboratory. *Can. Mineral.* **32**, 149-158.

MASAITIS, V.L., SHAFRANOVSKY, G.I., GRIEVE, R.A.F., PEREDERY, W.V., BALSAMOV, E.L. & FEDOROVA, I.G. (1997): Diamonds in suevites of the Sudbury impact structure, Canada. *Zap. Vser. Mineral. Obshchest.* **126**(4), 1-6.

MEURER, W.P. & BOUDREAU, A.E. (1996): An evaluation of models of apatite compositional variability using apatite from the Middle Banded Series of the Stillwater Complex, Montana. *Contrib. Mineral. Petrol.* **125**, 225-236.

MILKEREIT, B. & GREEN, A. (1992): Deep geometry of the Sudbury Structure from seismic reflection profiling. *Geology* **20**, 807-811.

MORRIS, W.A. (1984): Paleomagnetic constraints on the magmatic, tectonic, and metamorphic history of the Sudbury Basin region. *In* The Geology and Ore Deposits of the Sudbury Structure. *Ontario Geol. Surv., Spec. Vol.* **1**, 411-427.

NALDRETT, A.J. & HEWINS, R.H. (1984): The Main Mass of the Sudbury Igneous Complex. *In* The Geology and Ore Deposits of the Sudbury Structure. *Ontario Geol. Surv., Spec. Vol.* **1**, 235-251.

________, RAO, B.V. & EVENSON, N.M. (1986): Contamination at Sudbury and its role in ore formation. *In* Metallogeny of Basic and Ultrabasic Rocks (M.J. Gallagher, R.A. Ixer, C.R. Neary & H.M. Prichard, eds.). Institute of Mining and Metallurgy, London, U.K. (75-91).

NASH, W.P. (1976): Fluorine, chlorine, and OH-bearing minerals in the Skaergaard Intrusion. *Am. J. Sci.* **276**, 546-557.

PASTER, T.P., SCHAUWECKER, D.S. & HASKIN, L.A. (1974): The behavior of some trace elements during solidification of the Skaergaard layered series. *Geochim. Cosmochim. Acta* **38**, 1549-1577.

PEREDERY, W.V. & MORRISON, G.G. (1984): Discussions of the origin of the Sudbury Structure. *In* The Geology and Ore Deposits of the Sudbury Structure. *Ontario Geol. Surv., Spec. Vol.* **1**, 491-511.

PICCOLI, P.M. & CANDELA, P.A. (1994): Apatite in felsic rocks: a model for estimation of initial halogen contents in the Bishop Tuff (Long Valley) and Tuolumne Intrusive Suite (Sierra Nevada batholith) magmas. *Am. J. Sci.* **294**, 92-135.

ROELANDTS, I. & DUCHESNE, J.-C. (1979): Rare-earth elements in apatite from the layered norites and iron–titanium oxide ore-bodies related to anorthosites (Rogaland, S.W. Norway). *Phys. Chem. Earth* **11**, 199-212.

RØNSBO, J.G. (1989): Coupled substitution involving REEs and Na and Si in apatite in alkaline rocks from the Ilimanaussaq intrusion, South Greenland, and the petrologic implications. *Am. Mineral.* **74**, 869-901.

SHANNON, R.D. (1976): Revised effective ionic radii and systematic studies of interatomic distances in halides and chalcogenides. *Acta Crystallogr.* **A32**, 751-767.

SHAW, D.M., DOSTAL, J. & KEAYS, R.R. (1974): Additional estimates of continental surface Precambrian Shield composition. *Geochim. Cosmochim. Acta* **40**, 73-83.

STÖFFLER, D., DEUTSCH, A., AVERMANN, M., BISCHOFF, L., BROCKMEYER, P., BUHL, D., LAKOMY, R. & MÜLLER-MOHR, V. (1994): The formation of the Sudbury Structure, Canada: toward a unified impact model. *Geol. Soc. Am., Spec. Pap.* **293**, 303-318.

TACKER, R.C. & STORMER, J.C. (1989): A thermodynamic model for apatite solid solution applicable to high temperature geological problems. *Am. Mineral.* **74**, 877-888.

THOMPSON, L.M. & SPRAY, J.G. (1994): Pseudotachylitic rock distribution and genesis within the Sudbury Impact Structure. *Geol. Soc. Am., Spec. Pap.* **293**, 275-287.

THOMSON, M.L., BARNETT, R.L., FLEET, M.E. & KERRICH, R. (1985): Metamorphic assemblages in the South Range Norite and Footwall mafic rocks near the Kirkwood mine, Sudbury, Ontario. *Can. Mineral.* **23**, 173-186.

WALKER, R.J., MORGAN, J.W., NALDRETT, A.J., LI, CHUSI & FASSETT, J.D. (1991): Re–Os isotope systematics of Ni–Cu sulfide ores, Sudbury Igneous Complex, Ontario: evidence for a major crustal component. *Earth Planet. Sci. Lett.* **105**, 416-429.

WARNER, S. (1996): *Apatite in the Sudbury Igneous Complex, Ontario: Monitor of Fractionation, Degassing, and a Metamorphic Overprint.* M.Sc. thesis, McGill Univ., Montreal, Quebec.

WATSON, E.B. (1980): Apatite and phosphorus in mantle source regions: an experimental study of apatite/melt equilibria at pressures to 25 kbar. *Earth Planet. Sci. Lett.* **51**, 322-335.

________ & GREEN, T.H. (1981): Apatite/liquid partition coefficients for the rare earth elements and strontium. *Earth Planet. Sci. Lett.* **56**, 405-421.

Received September 12, 1996, revised manuscript accepted June 30, 1998.